

## Design of load-to-failure tests of high-voltage insulation breaks for ITER's cryogenic network

This content has been downloaded from IOPscience. Please scroll down to see the full text.

2015 IOP Conf. Ser.: Mater. Sci. Eng. 102 012009

(<http://iopscience.iop.org/1757-899X/102/1/012009>)

View [the table of contents for this issue](#), or go to the [journal homepage](#) for more

Download details:

IP Address: 137.138.125.164

This content was downloaded on 14/04/2016 at 10:53

Please note that [terms and conditions apply](#).

# Design of load-to-failure tests of high-voltage insulation breaks for ITER's cryogenic network

S.A.E.Langeslag<sup>1</sup>, E.Rodriguez Castro<sup>1,2</sup>, I.Aviles Santillana<sup>1,3</sup>,  
S.Sgobba<sup>1</sup>, A.Foussat<sup>4</sup>

<sup>1</sup> CERN, CH-1211 Genève - Switzerland

<sup>2</sup> University of Vigo, Campus de As Lagoas-Marcosende, 36310 Vigo - Spain

<sup>3</sup> University Carlos III of Madrid, Campus de Leganes, 28911 Madrid - Spain

<sup>4</sup> ITER Organization, Route de Vinon sur Verdon, CS 90 046, 13067 St. Paul lez Durance Cedex - France

E-mail: Stefanie.Langeslag@cern.ch

**Abstract.** The development of new generation superconducting magnets for fusion research, such as the ITER experiment, is largely based on coils wound with so-called cable-in-conduit conductors. The concept of the cable-in-conduit conductor is based on a direct cooling principle, by supercritical helium, flowing through the central region of the conductor, in close contact with the superconducting strands. Consequently, a direct connection exists between the electrically grounded helium coolant supply line and the highly energised magnet windings. Various insulated regions, constructed out of high-voltage insulation breaks, are put in place to isolate sectors with different electrical potential. In addition to high voltages and significant internal helium pressure, the insulation breaks will experience various mechanical forces resulting from differential thermal contraction phenomena and electro-magnetic loads.

Special test equipment was designed, prepared and employed to assess the mechanical reliability of the insulation breaks. A binary test setup is proposed, where mechanical failure is assumed when leak rate of gaseous helium exceeds  $10^{-9} Pa \cdot m^3/s$ . The test consists of a load-to-failure insulation break charging, in tension, while immersed in liquid nitrogen at the temperature of 77 K. Leak tightness during the test is monitored by measuring the leak rate of the gaseous helium, directly surrounding the insulation break, with respect to the existing vacuum inside the insulation break. The experimental setup is proven effective, and various insulation breaks performed beyond expectations.

## 1. Introduction

Magnet systems for plasma confinement, in fusion energy experiments such as ITER, include a wide range of coils composed of cable-in-conduit conductors (CICCs) [1]. These CICCs consist of various types of stainless steel jackets, densely filled with superconducting strands based on either Nb<sub>3</sub>Sn or NbTi, and subsequently compacted [2]. Cooling, necessary for the operation of these superconducting cables, is realised by direct passage of supercritical helium through the conduits, thereby directly mitigating heat at the superconducting strands. This concept provides a highly efficient cooling scheme by a concentrated liquid helium supply from the cryogenic circuit to the superconducting strands [3], however it intrinsically connects the high-current pulsed coils to the helium supply pipes of the cryogenic distribution system.



High-voltage insulation breaks (IBs) provide the required electrical isolation between the CICC and the helium supply pipes, to prevent a direct electrical connection between high-current coils and the electrically grounded cryogenic supply system [4]. The IBs will be situated at the helium inlet and outlet channels of the wide range of parallel cryogenic circuits foreseen in the ITER magnet system. A large number, over 1000, of these electrical separation units will therefore be indispensable for a successful operation of the tokamak. These axial insulation breaks are built up from stainless steel end-fittings, hermetically connected via a glass-reinforced resin composite body of sufficient length, to prevent electrical discharge during magnet operation (figure 1).

The IBs do not only have to comply with electrical requirements, but also sustain demanding conditions resulting from elevated mechanical stress originating from electro-magnetic loads, dilatation effects and high internal pressure during magnet operation [4]. Therefore the cryogenic insulation system does not only rely on the electrical, but also the structural properties of the individual IBs.

To validate the state of the art IBs and check their ability to withstand the highly demanding operating conditions, a binary test setup is proposed. An experimental setup was designed, manufactured and commissioned, allowing for an extensive assessment of the structural reliability of currently produced IBs. Additionally the results are presented of measurements obtained for certain IBs tested according to this procedure.

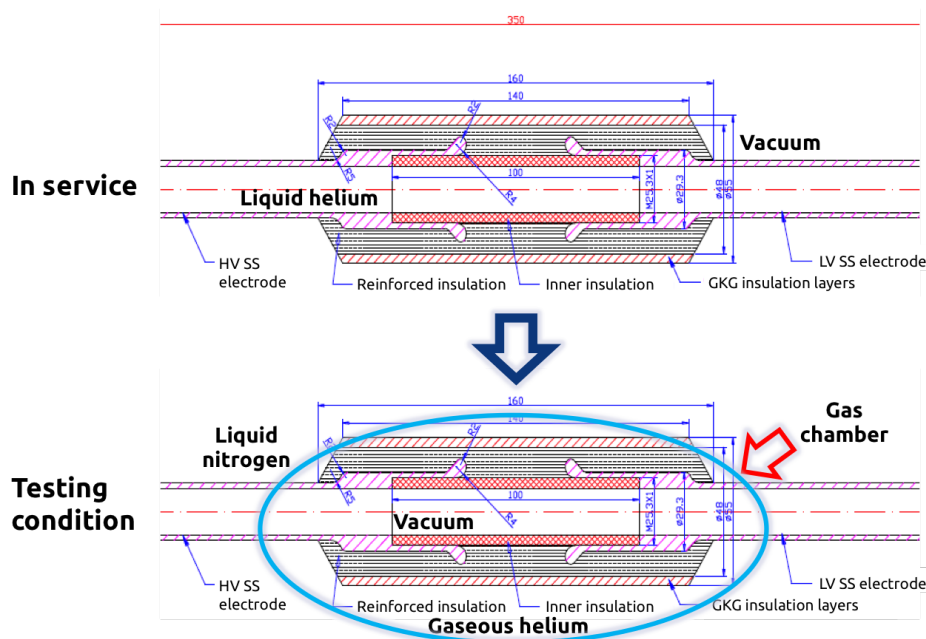


Figure 1: Technical drawing of a 30 kV insulation break, demonstrating the environmental conditions during operation and testing, respectively. Note that the cooling scheme in testing condition is reversed with respect to the operating condition.

## 2. Materials

Commissioning tests of the experimental setup involved a smaller type 4 kV break type, while subsequent tests, presented in § 4, were performed on 30 kV IBs with dimensions described in figure 1. All priorly described IBs, denoted as IB4kV, IB30kV1 and IB30kV2, respectively, were formerly tested up to very low loads, max. 2 kN, in a single traction-compression test [5]. These test items can therefore not be considered to be in a fully pristine state.

### 3. Experimental setup

A test system has been developed for reliability testing of individual IBs during magnet operation. The IBs structural integrity is challenged by applying increasing load while monitoring its leak-tightness to gaseous helium. Mechanical loads in the IBs, originating from dilatation effects and electro-magnetic forces, include tensile, bending and torsional components. As a result of the large share of the tensile component derived from the alternating hoop forces in the pulsed coils, increased by possible thermal contraction effects, the loading scenario during IB testing has been chosen uniaxial in tension.

Some of the mechanical loads will be introduced during magnet commissioning, in essence cool-down between 293 K and 4 K, however some of them will also occur while at the 4 K operating temperature. To take into account temperature effects the measurements are performed at cryogenic temperature, here liquid nitrogen temperature (i.e. 77 K) to avoid closed-circuit complications to be encountered when testing at liquid helium temperature (i.e. 4 K). In the measurements mechanical failure is assumed when the leak rate exceeds  $10^{-9} Pa \cdot m^3/s$ .

#### 3.1. Sample adjustment

To adapt the IBs in order to apply the testing load scenario, modifications are made to both extremities of the as-received IBs. On one extremity a small flange Gyrolok<sup>®</sup> coupling is TIG welded, with a Böhler ASN 5-IG (material number 1.4453) filler wire, to the IB helium pipe via a U-shaped tube to allow easy access for pumping. The connection between this vacuum tube (U-tube) and the IB's stainless steel end fitting is realised via an increased diameter thick ring which acts as a load bearing surface during tensile testing.

On the other extremity a lap joint TIG weld was realised with the same filler metal between the IB end fitting and a threaded rod for top-end IB fixation to the universal testing machine in order to allow for load transmission. These adaptations have been performed in a manner to guarantee their mechanical integrity and leak tightness to avoid any influence on the outcome of the tests. Computed radiographic inspections have been performed on the welded extensions with a Philips MG161L 160 kV + MCN 166 X-ray tube, according to examination standard EN 14784-2 class B. All welds were established to conform to EN ISO standard 5817, level B. Additionally, two PT100 temperature sensors are placed on each IB, on the stainless steel end-fittings adjacent to the glass-resin composite body, in order to monitor real-time temperature at the sample.

#### 3.2. Setup design features

The objective of the measurement is to test the IBs in traction at 77 K while monitoring leak tightness, and identifying the load at which the leak rate exceeds the imposed value of  $10^{-9} Pa \cdot m^3/s$ .

To this aim, the cooling scheme of the insulator break is inverted. Where in service condition a vacuum exists around, and liquid helium flows through the IB, in testing condition a vacuum is created inside the IB and it is cooled externally. This concept, shown in figure 1, is adopted for a better vacuum achievement and a leak rate reading on the vacuum pump solely influenced by the IB's structural integrity, hence avoiding environmental impact.

The setup consists of a G10 open liquid nitrogen cryostat to realise a measurement process at 77 K. Low density gaseous helium is employed as flow agent for leak detection, for which a gas dome is employed directly surrounding the to be measured IB. The gas dome is supported from the IB via a small fraction of the top end sample thread. The weight of the dome is minimised by constructing it out of a low density aluminium alloy, as to limit external factors on the measurement results. Moreover, the cross-section of the dome is limited, to realise an as

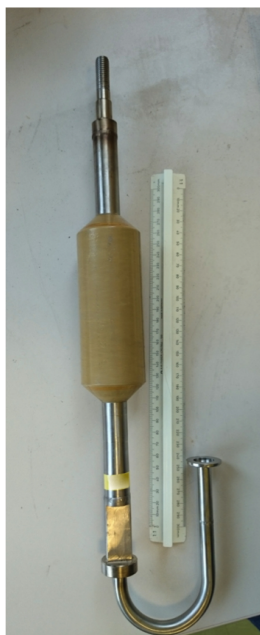


Figure 2: Insulation break sample, adjusted for load-to-failure testing.



Figure 3: Adjusted insulation break sample including attached tooling for load and vacuum application.



Figure 4: Adjusted insulation break sample including attached tooling for load application and gas dome.

direct as achievable cooling at the position of the IB, i.e. to reduce the gaseous column between the IB and its coolant, for which the highly thermally conductive Al-alloy is also beneficial.

The bottom tooling is designed to grip around the load bearing ring on the bottom end of the sample, while simultaneously allowing for the passage of the vacuum tube (U-tube). Vacuum inside the IB is obtained with use of a Leybold, PhoenixXL 300, mass spectrometer pump, on which the leak rate during testing is consistently monitored.

Measurements are performed on a UTS200 universal tensile/compression machine, from UTS Testsysteme GmbH. The machine can reach a maximum force of 200 kN with a position accuracy (stroke displacement) of  $1 \mu\text{m}$ . Load is registered with use of a HBM Z12, 200 kN load cell with 0.0016 kN resolution. The test procedure is programmed in DionPro software via which the system is subsequently actuated and the load versus displacement data is recorded. Temperature data is registered via a QuantumX DAQ system through Catman software on a parallel computer.

### 3.3. Experimental procedure

An initial leak check of the IB sample is performed, by pumping vacuum inside the IB sample followed by the passage of pressurised gaseous He around the sample. The initial leak checks performed have been satisfactory for all measured IBs. Following cryostat mounting and subsequent IB sample including gas dome fixation, the sample is vacuumised. Generally a leak rate level is reached better than  $10^{-11} \text{Pa} \cdot \text{m}^3/\text{s}$  prior to thermalisation (better than  $10^{-13} \text{Pa} \cdot \text{m}^3/\text{s}$  at 77 K prior to testing). Subsequently liquid nitrogen is introduced into the cryostat and owing to the dome shaped gas shell and thus its unsealed bottom, a direct flow of nitrogen at the IB sample is realised. Once full thermalisation is achieved, resulting from complete submersion of the IB sample, gaseous He is introduced in the dome. This is done by means of introducing pressurised

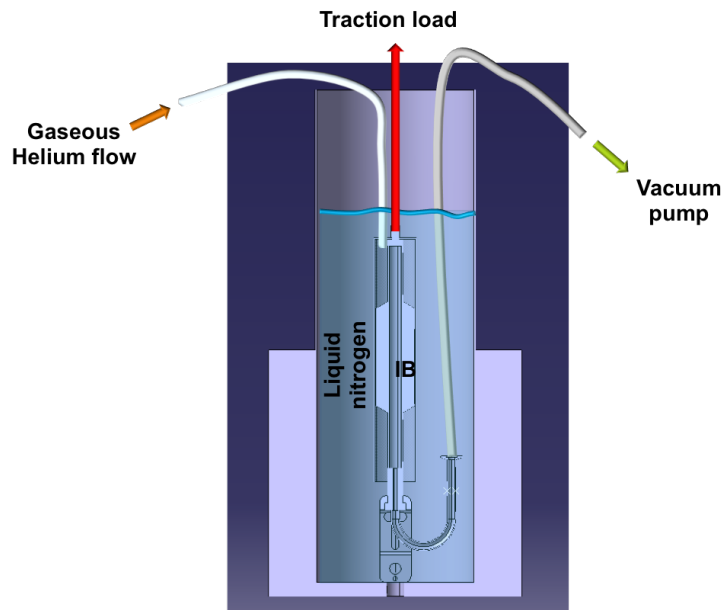


Figure 5: Schematic diagram illustrating the binary test setup design. Note the gaseous helium, directly surrounding the insulation break with internal vacuum, immersed in liquid nitrogen.

gas from the top of the dome, consequently expelling the liquid nitrogen from the bottom. The introduction of the gaseous helium around the IB sample offers a final leak check prior to loading.

A dual test procedure is implemented, consisting of a primary and a secondary test. The primary test holds the load-to-failure measurement, while in the secondary test the nature of the introduced damage is examined. For both tests a low frequency cyclic loading scheme was adopted to discriminate reversible from irreversible flaws. Five consecutive cycles are carried out, where after each cycle load was released down to 2 kN. The loading scheme includes successive cycles to 5 kN, 10 kN, 15 kN, 30 kN and 85 kN, with a loading speed of 50 N/s in both the loading and unloading segment. Charging was interrupted promptly at leak detection to avoid any damage to the mass spectrometer pump.

#### 4. Discussion of selected test results

##### 4.1. Primary test

Data for the primary measurements of two typical 30 kV IBs is presented in figure 6 and 7. The plots represent the leak rate over time, as recorded by the mass spectrometer pump, and the load applied, respectively. The plots show a very consistent behaviour between the two IBs, IB30kV1 and IB30kV2, where early in the load-cycles a rapid increase in leak rate is observed, whereas during the third load cycle the leak rate stabilises.

In both cases, during the fifth load cycle, up to 85 kN, a very sudden rise in leak rate is observed, passing rapidly beyond the imposed failure level. The cycle was immediately interrupted at the recorded sample breakdown to avoid any damage to the mass spectrometer pump. The load at which failure is noted is  $\sim 65$  kN and  $\sim 71$  kN, for IB30kV1 and IB30kV2, respectively. These values exceed by far the expected performance of such cryogenic insulation breaks, which lies a factor ten below.

Primarily at the onset of the measurement, some noise is observed in the leak rate for both sample IB30kV1 and IB30kV2. An assumption is made that the observed spikes in the leak rate curve appear as a result of internal pollution inside the IB, present prior to testing. Samples have not been specifically prepared for vacuum application, and can therefore contain some particles which can interfere with the leak rate reading of the mass spectrometer pump. For future application of the test procedure a preparation as such may be beneficial.

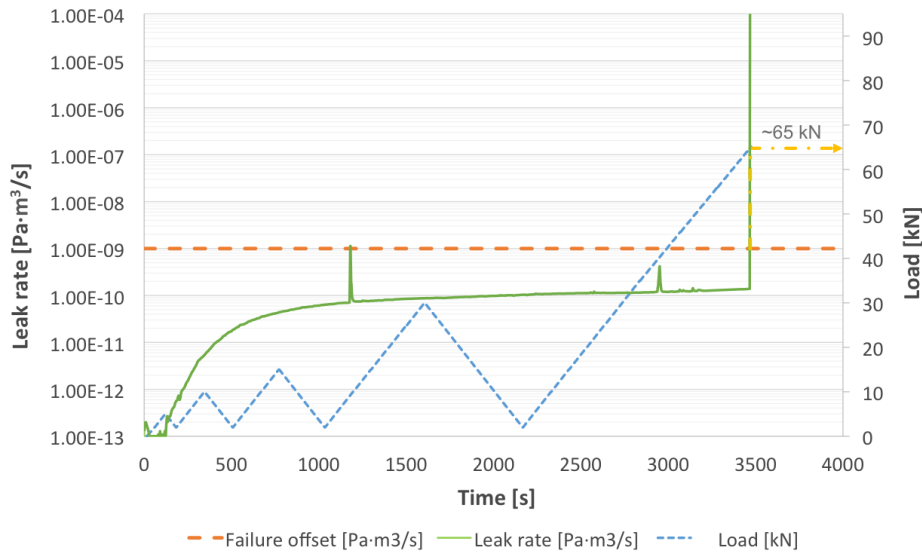


Figure 6: Diagram showing the leak rate and applied load over time for the primary load-to-failure test of IB30kV1 at 77 K, measured following the presented loading procedure. Breakdown was recorded at  $\sim 65$  kN.

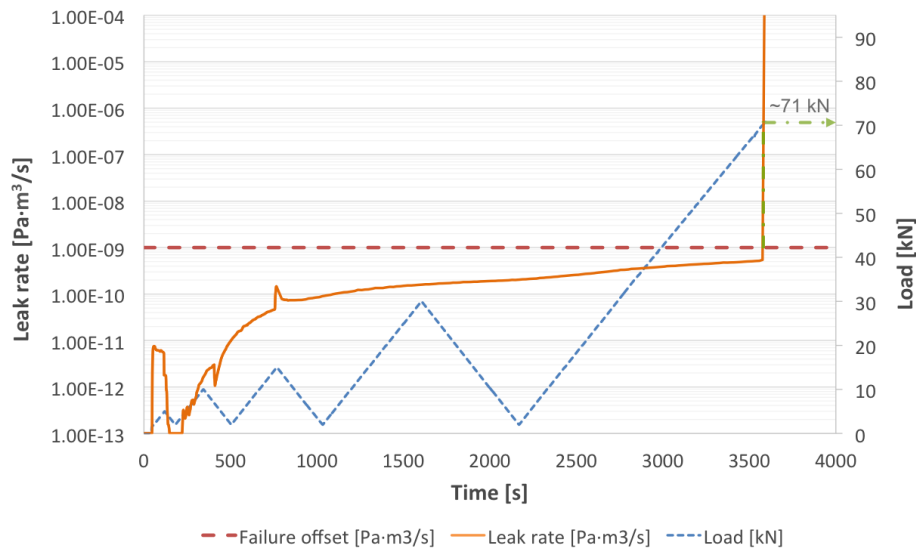


Figure 7: Diagram showing the leak rate and applied load over time for the primary load-to-failure test of IB30kV2 at 77 K, measured following the presented loading procedure. Breakdown was recorded at  $\sim 71$  kN.

#### 4.2. Secondary test

An additional test was performed, following the load-to-failure test, aimed at confirming breakdown and discriminating between reversible and irreversible defects. The leak rate over time, versus the applied load cycles for this secondary test, presented in figure 8 shows a leak rate directly related to the applied load. The leak rate changes abruptly with load, demonstrating a partially reversible feature of the induced defect during the primary test. The imposed failure level is now however exceeded at a significantly lower load, i.e. at  $\sim 13$  kN, at which the permanent leak becomes apparent.



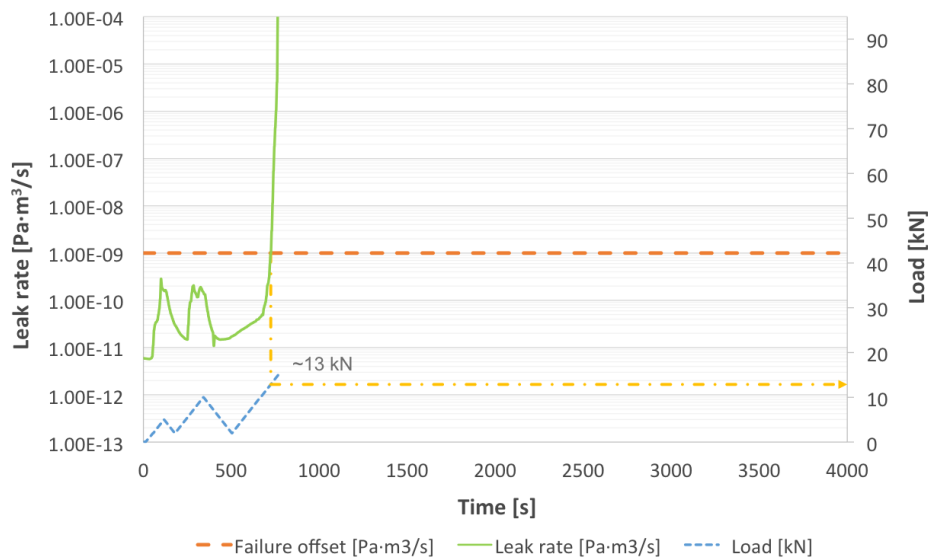


Figure 8: Diagram demonstrating leak rate and applied load over time for the secondary test of IB30kV1 at 77 K. At low applied loads one can note a reversible feature of the leak introduced during the primary test.

#### 4.3. Observed defects

Visual inspection, following the measurements, demonstrated signs of damage on the sample, as shown in figure 9. The damage is located primarily at the interface between the stainless steel end fittings and the first glass-resin layer, or amidst the glass-resin layers, in an interlayer fashion. These defects become more apparent after applying a liquid penetrant followed by a revelator, during penetrant testing (PT), which can be witnessed in figure 10. The image shown is obtained 30 minutes following the application of the revelator, according to ISO standard 3452-1.



Figure 9: Defective regions observed on the as-tested IB30kV2, by visual inspection.



Figure 10: Observation of defective regions on IB30kV2, revealed by the application of liquid penetrant.



## 5. Conclusion

A binary test setup was successfully designed, developed and commissioned for load-to-failure tests of axial insulation breaks at cryogenic temperature. Failure was reached, by applying a tensile load until a certain leak rate threshold was exceeded, which was set at  $10^{-9} Pa \cdot m^3/s$ . Following an initial test campaign, a good test reproducibility was obtained for all the tests performed.

During a primary load-to-failure test, the insulation break samples fail consistently at high tensile loads, i.e.  $\sim 65$  kN and  $\sim 71$  kN for the examples IB30kV1 and IB30kV2 presented, respectively. Failure is accompanied by an extensive damage of the insulation breaks, in an interlayer fashion, and at the interface where the stainless steel end-fitting and the glass-resin composite meet.

Secondary tests, implemented to examine the nature of the introduced damage, have demonstrated that a part of the damage is reversible. It has been noted that with temperature as a result of dilatation differences during cool-down, and with small load increments, damage opens and closes, thereby increasing and decreasing leak rate, respectively. Above a certain load, far below the load necessary for failure during primary testing, the irreversible damage becomes apparent when leak rate increases abruptly beyond the imposed threshold of  $10^{-9} Pa \cdot m^3/s$ .

### 5.1. Disclaimer

The above conclusions arise from a limited sample basis, hence they cannot be considered as sufficiently exhaustive to guarantee the performance of the axial insulation breaks at operating conditions, i.e. at supercritical helium temperature and in a repeated loading condition.

*The views and opinions expressed herein do not necessarily reflect those of the ITER Organization.*

## 6. References

- [1] N. Mitchell, A. Devred, P. Libeyre, B. Lim, and F. Savary, "The ITER Magnets: Design and Construction Status," *IEEE Transactions on Applied Superconductivity*, vol. 22, no. 3, pp. 4200809–4200809, 2012.
- [2] B. Turck, D. Bessette, and D. Ciazynski, "Design methods and actual performances of conductors for the superconducting coils of Tokamaks," *Fusion Engineering and Design*, vol. 2, pp. 667–670, 1993.
- [3] L. Bottura and C. Luongo, "Superconductors, stability in forced flow," *Wiley Encyclopedia of Electrical and Electronics Engineering*, 1999.
- [4] F. Rodriguez-Mateos, D. Evans, and A. Devred, "Essential design, construction and test elements of ITER axial insulation breaks," *Transactions of the International Cryogenic Materials Conference ICMC*, 2014.
- [5] J. Kosek, R. Lopez, F. Rodriguez-Mateos, and D. Tommasini, "Non-destructive qualification tests for ITER cryogenic axial insulating breaks," in *AIP Conference Proceedings*, pp. 1026–1033, Jan. 2014.